International Journal of Fluid Power 4 (2003) No. 3 pp. 5-15

HYDRAULIC BRIDGE FOR PRESSURE CONTROL IN A P-Q MULTIPLE LINE SEGMENT CONTROL VALVE

Richard Burton[1], Jian Ruan[2] and Paul R. Ukrainetz[1]

[1]*Department of Mechanical Engineering, University of Saskatchewan, 57 Campus Drive, Saskatoon, Saskachewan, Canada, S7N 5A9*
burton@engr.usask.ca
[2]*Department of Mechanical Engineering, Zhejiang University of Technology, Hangzhou 310014, P.R. China*
wxmin@public.hz.zj.cn

Abstract

The conventional device for flow rate and pressure multiple control is a combination of a flow rate valve and a pressure relief valve. For the pressure control, a hydraulic bridge can also be used instead of using a pressure relief valve. In this paper, a special hydraulic bridge was developed to undertake pressure control in a pressure compensated flow rate valve and thus a new type of P-Q control valve is constructed. The pressure control in this P-Q control valve is a hydraulic bridge formed by the serial connection between a metering orifice and a drain orifice. The contour of the valve port has a significant effect on the linearity of the output pressure. Theoretical analysis shows that the linear pressure output characteristic corresponds to a valve port contour of a hyperbolic. Due to the difficult machining of this hyperbolic contour, a multiple line with two segment lines is used to approximate the valve port contour for linear pressure output. The pressure bridge is constructed in a 2D P-Q control valve and an experimental investigation is carried out. It is demonstrated that linearity of the output pressure is greatly improved by using the multiple segment line contour of the valve port and it is demonstrated that the output pressure is not sensitive to the variation of the temperature. With the introduction of the pressure control bridge, the P-Q valve is indeed greatly simplified.

Keywords: flow rate and pressure multiple control, pressure compensated flow valve, contour of valve port, linearity

1 Introduction

Many industrial applications using fluid power systems require the actuators to control force (torque) and speed alternately. As an example, a conventional system for speed and force control is demonstrated in Fig. 1. During initial positioning of the cylinder piston, speed control is required. In many applications, a pressure compensated flow rate valve can be sufficiently accurate (high motion stiffness) for this purpose. As the piston approaches and makes contact with the workpiece, a pressure limiting device (in this case, a relief valve) is used to control the pressure and thus the output clamping force. In applications which use multiple actuators, all of which require speed and force control, directional control valves can be placed between the cylinder and flow control valve to direct the desired flow rate to the actuator being controlled.

An injection molding machine is one such example (Zheng et al, 1980). The pump and appropriate valves must deliver fluid first to a driving cylinder whose speed is controlled at a preset value for the opening and the closing of the molds (flow control). The circuit then ports fluid to a second cylinder which is connected to the barrel of a screw type pump. Slow movement of the pump barrel is used to maintain a constant pressure during the injection and cooling down cycles (Xie, 1990). Thus, the hydraulic system requires pressure control during this part of the cycle. In most applications, two valves are used to achieve these two distinctly different control functions. A pressure compensated flow control valve is used to control the velocity of the opening or closing part of the process. For energy efficiency, the flow control valve is often of the bypass flow variety. A relief valve is used for the pressure control. This kind of multi-functional (mode) system is called a P-Q hydraulic circuit.

In other types of P-Q circuits, the dual modes of pressure (force) or flow rate control (speed) can also be achieved using electrical feedback signals. The force or speed of the actuator is controlled by feeding back measured force or speed signals to a computer controller which then sends an appropriate signal to drive a single servo valve in a closed loop mode (Cai et al, 1999). A one-chip computer and electrical feedback

This manuscript was received on 14 April 2003 and was accepted after revision for publication on 06 October 2003

signals were used to control pressure and flow in a single valve. Generally, the electrical version of the P-Q control circuit is more flexible than its mechanical counterpart in its control strategy, but the system tends to be complex in structure and expensive in cost.

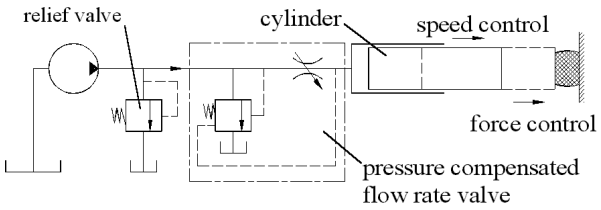

Fig. 1: *Hydraulic P-Q multiple function system (conventional)*

For many applications, pressure control and pressure modulation can also be achieved using a resistance bridge in conjunction with a pressure limiting valve. Compared to a pressure control valve, the resistance bridge is simple in structure and relatively inexpensive (Backé, 1973). A limiting problem with resistance bridges is that they are sensitive to changes in the flow rate. However, in most applications in which a P-Q control valve is used, the pressure control is required only when the actuator comes to a stop. In this case, the flow rate is very small. The application of the resistance bridge for pressure control thus becomes feasible.

A challenge in undertaking pressure control using a flow control valve is a consequence of the nonlinear square root relationship between the flow and the pressure drop across the throttling orifice. A common approach has been to integrate "notches" in the spool lands which improves the linearity about the null position of the spool; indeed, the flow rate can be made approximately linear with opening area (the pressure drop across the orifice being held constant through the use of an hydrostat). Thus, the flow rate can be estimated using a displacement transducer located on the spool (Lu et al, 1986). In a pressure control system with constant delivery pump and bypass throttling valve, the opening of the throttling valve can also be designed to yield a linear relationship between the pressure and the displacement of throttling spool (Cai et al, 1999). In some cases, the load pressure is fed to the valve to accomplish pressure control which increases the damping ratio. Other approaches use actual measurements of flow rate and pressure feedback to control an electro-hydraulic proportional valve to switch between the two desired functions (Li, 1993).

In this paper, a hydraulic bridge is integrated into a single valve which has a dual mode function (P-Q). Because it is usually necessary to change the pressure in response to some controlling signal, a means of achieving this through changing one of the resistances of the bridge is introduced. The paper considers the design of the lands of the metering orifice of a bypass flow control valve; for a certain spool land's displacement range, the orifice facilitates flow control and for another range, the orifice becomes one of the resistances in the bridge. For the Q function, the metering orifice is of standard form; in the P mode, the lands both for the metering-in and metering-out valve opening are contoured to provide a linear relationship between spool land displacement and pressure. Thus, the pressure can be linearly controlled by varying the displacement of the spool. An experimental P-Q valve has been fabricated and its characteristics evaluated. The linear performance of the pressure control vs spool land displacement is demonstrated by the experimental system.

2 Hydraulic Bridge in the P-Q Valve

A P-Q valve is illustrated in Fig. 2. For $x_p \le x_v < x_f$, the metering orifice is of a conventional type. Flow (Q) control is accomplished through pressure compensation via the bypass hydrostat. When the valve is to be used for pressure (P) control, the spool operates in the region $0 \le x_v < x_p$. For the application in mind, the load resistance is significant (very little flow). It should be noted that very small metering notches have been integrated at the extremities of the spool lands as illustrated. As will be illustrated, these metering notches are specially contoured to provide specific area gradient characteristics. An equivalent hydraulic bridge circuit of the metering notches is shown in Fig. 3 for the condition of $0 \le x_v < x_p$.

Before proceeding, it must be pointed out that to demonstrate the concept of the hydraulic bridge, the notches shown in Fig. 2 are contoured on the spool lands. The notches can also be machined into the spool ports in the sleeve. However, since the concept is easier to illustrate if the lands are shown countered, the configuration shown in this figure is adopted for explanation purposes. The principle of operation and describing equations are identical for both cases.

For $x_v = 0$, the flow from the ps port to the load port is blocked. However, there exists a path from the load port to tank via the contoured spool land as indicated (drain orifice). When the spool is actuated in the region $0 \le x_v < x_p$, fluid is ported from the ps port through the notched orifice (upstream orifice) to the load port (Q1). Because the resistance of the load is very high, negligible flow to the load occurs; thus fluid passes through the second notched orifice to tank (Q2). The two notches, therefore, form the two arms in the hydraulic pressure bridge.

In the region $0 \le x_v < x_p$, the flow through each arm is the same (no flow to the load). Further, since the objective is to vary the load pressure in a linear fashion vs the spool displacement, and because the pressure drop across the first metering orifice is fixed (via the hydrostat), then the flow through the two resistance arms is constant and independent of the load pressure.

In order to demonstrate how the pressure bridge works, it is necessary to develop some describing equations. Consider Fig. 2 and Fig. 3. The flow rate through the upstream notched orifice is

$$Q_1 = C_d A_r \sqrt{\frac{2(p_s - p_L)}{\rho}} \qquad (1)$$

The flow rate through the drain orifice is given by

$$Q_2 = C_d A_l \sqrt{\frac{2p_L}{\rho}} \tag{2}$$

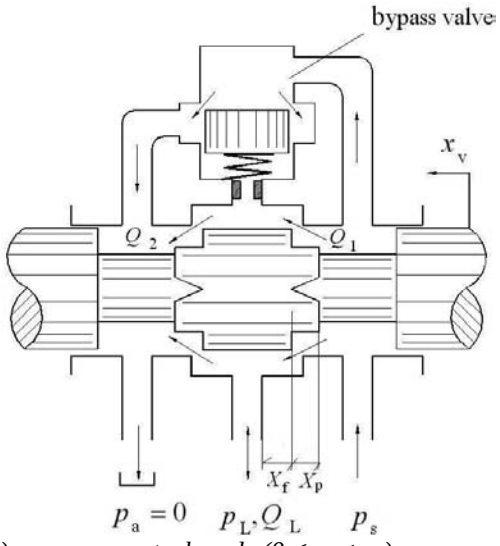

(a) pressure control mode ($0 \le x_v < x_p$)

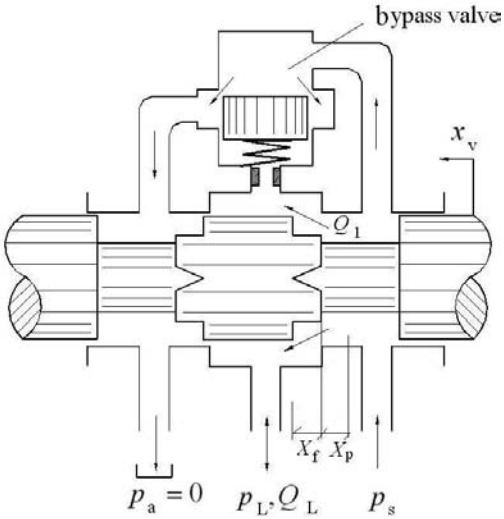

(b) flow rate control ($x_p \le x_v < x_f$)

Fig. 2: *P-Q Valve*

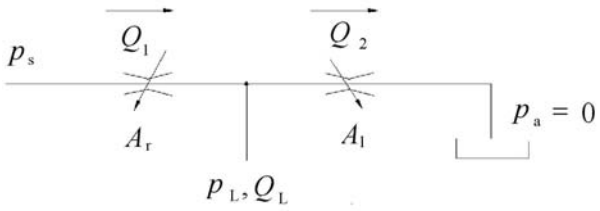

Fig. 3: *Equivalent circuit of the resistance bridge*

It should be noted that the flow rate through the bridge is, in fact, laminar. However, the square root relationship is convenient to use for consistency in this situation. It is recognized that the discharge coefficient is not constant and strongly dispends on the Reynolds number. The flow rate through the bypass valve is

$$Q_b = C_d A_b \sqrt{\frac{2p_s}{\rho}} \tag{3}$$

and the flow for the hydraulic bridge is given by

$$Q_1 - Q_2 = Q_L \tag{4}$$

Because flow to the actuator is negligible,

$$Q_1 = Q_2 \tag{5}$$

The continuity equation of the pump is given by

$$Q_p - K_l p_s = Q_1 + Q_b \tag{6}$$

In the above equation, K_1 is the leakage coefficient of the pump.

Consider Fig. 2. The force balance equation of the bypass valve spool is given by

$$A_{sb}(p_s - p_L) = K_s(X_0 + x_b) + F_b + F_f \text{sign}(x_b') \tag{7}$$

In the above equation, F_b is the flow force and F_f is the Coulomb frictional force. Equations 1 through 7 can now be used to demonstrate how pressure control can be realized with the hydraulic bridge.

Consider Eq. 7, to ensure that the flow control is independent of the load pressure, the value of spring precompression X_0 is usually designed to be much larger than the maximum displacement of the bypass valve spool x_{bmax}. For this reason, the variation of spring force caused by the change of spool's displacement is negligible. Furthermore, compared to the hydrostatic forces on the two end faces of the bypass valve spool, flow forces, F_b, and Coulomb frictional forces, F_f, are usually small enough to be disregarded. Equation 7 can be simplified to

$$A_b(p_s - p_L) = K_s X_0 \tag{8}$$

Since p_s - p_L is a constant and is the pressure drop across the flow control metering orifice, then flow across the orifice is constant.

In the development of the relationship between the load pressure p_L and the spool's displacement x_v, an important assumption is made that the flow coefficients C_d for the control metering orifice and the drain orifice are the same. C_d is strongly dependent on the Reynolds Number in the low Reynolds number region. However, in the hydraulic pressure control bridge, the change in the Reynolds Number when the load pressure varies is approximately the same for the control metering orifice and drain orifice. Hence, any changes in C_d for either orifice are about the same and hence their effects cancel out. For simplification purposes, the discharge coefficient C_d for the control metering orifice and the drain orifice is assumed to be the same value.

Upon some manipulation of Eq. 1 through 8, p_L vs the displacement x_v can be given as

$$p_L = \frac{A_r^2(x_v)}{A_l^2(x_v)} \frac{K_s X_0}{A_b} \tag{9}$$

In this equation, $(K_s \cdot X_0)/A_b$ is a constant. It can be observed from Fig. 2 that A_r and A_l are related to the displacement of the spool x_v. Through a judicious choice of the geometry of the orifice areas, the desired

linear output of pressure as a function of the spool's displacement is possible. This is critical to the success of this valve's performance. The design of the notch geometry of the two orifices is now considered.

3 Design of the Valve Ports

3.1 Valve Port for Linear Pressure Output

From Eq. 9, it is seen that the geometric shape of the valve ports has an effect on the control pressure p_L. In order to keep the machining cost of the notches down, the upstream port metering orifices should have the same geometric shape as that of the drain orifices. Consider Fig. 4 which shows two possible methods of orienting the two notches. Figure 4(a) illustrates the case when the notches have the same orientation in the axial direction. Figure 4(b) shows the case where the two notches are oriented in the oppose direction in the axial direction. The triangular notch is chosen only for illustration purposes. It should be noticed in the illustration that the valve opening area is formed between the notch and the straight edge of the groove on the sleeve (dotted line in Fig. 4). To accommodate machining, the notch can be fabricated on the sleeved while keeping the edge of spool land straight.

It should be recalled that the objective behind the design of the notch geometry was to ensure that the load pressure was linear with spool displacement in the region $0 < x_v < X_p$. That is, $p_L = k \cdot x_v$.

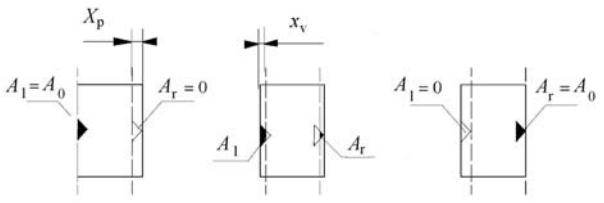

(a)

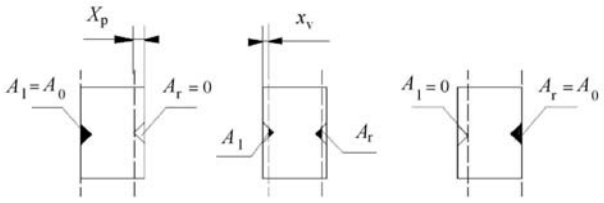

(b)

Fig. 4: *Relative positions of the valve ports*

This relationship is next expressed in a normalized form. By defining $\bar{x}_v = x_v / X_p$ and $\bar{p}_L = p_L / p_{max}$, then

$$\bar{p}_L = \bar{x}_v \tag{10}$$

For the case of Fig. 4(a), the relationship between the opening areas of the metering orifice and the drain orifice can be expressed as

$$A_1 = A_0 - A_r \tag{11}$$

where A_0 is the area of the uncovered orifice.

Substituting Eq. 10 and 11 in Eq. 9 yields

$$p_L = \frac{\bar{A}_r^2}{(1 - \bar{A}_r^2)^2} \; K_s X_0 / A_b \tag{12}$$

where $\bar{A}_r = \frac{A_r}{A_0}$.

By substituting $p_L = p_{max}$ (x_v / x_{vmax}) into Eq. 12 and solving for $\bar{x}_v$ as a function of $\bar{A}_r$, the valve port area which will force the pressure to satisfy $p_L = p_{max}$ (x_v / x_{vmax}) can be found as

$$\bar{A}_r = \frac{\sqrt{K\bar{x}_v}}{1+\sqrt{K\bar{x}_v}} \tag{13}$$

where $K = p_{max} / (p_s - p_L) = p_{max} A_{sb} / (K_s X_0)$.

The orifice area gradient is thus found by differentiating $\bar{A}_r$ with respect to $\bar{x}_v$ to yield

$$W = f(\bar{x}_v) = A_r' = \frac{KA_0}{2X_p\sqrt{K\bar{x}_v}(1+\sqrt{K\bar{x}_v})^2} \tag{14}$$

Equation 14 indicates that the orifice area gradient of the orifice is a function of the spool displacement. In non-dimensional form, Eq. 14 can be written as

$$\bar{W} = \frac{WX_p}{A_0} = \frac{K}{2\sqrt{K\bar{x}_v}(1+\sqrt{K\bar{x}_v})^2} \tag{15}$$

Equations 10, 13 and 15 can be plotted as a function of the spool displacement, $\bar{x}_v$, as shown in Fig. 5. This is how the area gradient of the notched orifices must appear if p_L is to be linear in x_v. Thus, the challenge remains one of finding a simple geometry that will satisfy the area relationship in this figure. It must be emphasized that, graphically, the shape which the area gradient forms in Fig. 5 is, in fact, the desired shape of half of the metering notch. Thus, this complex shape would have to be machined into the spool sleeve at the ports.

Consider the second configuration shown in Fig. 4(b). For the case of Fig. 4(a), the relationship between opening areas of the metering valve port and the drain valve port can be expressed as

$$A_r(\bar{x}_v) = A_1(1-\bar{x}_v) \tag{16}$$

Note that in Eq. 16, $A_1(1-\bar{x}_v)$ is a functional relationship, not a product.

Substituting Eq. 10 and 15 into Eq. 9, the valve port corresponding to the linear pressure output can be obtained as

$$\frac{a(\bar{x}_v)}{a(1-\bar{x}_v)} = \sqrt{K\bar{x}_v} \tag{17}$$

For the configuration shown in Fig. 4(b), it can be shown that a linear pressure output with respect to $\bar{x}_v$ can never be obtained through any geometrical shape of the orifices. This is shown as follows. Consider Eq. 16. Assume $\bar{x}_v = a$ and $\bar{x}_v = 1-a$ where $a \in (0,1)$. Then

$\frac{a(a)}{a(1-a)} = \sqrt{Ka}$ and $\frac{a(1-a)}{a(a)} = \sqrt{K(1-a)}$. Multiplying these two equations yields $K\sqrt{a(1-a)} = 1$. This equation must be satisfied in the given region. Now, when the valve displacement a is within the area (0, 1), the value of $K\sqrt{a(1-a)}$ is not constant but varies. Therefore, the equation $K\sqrt{a(1-a)} = 1$ is not tenable in this region. Thus it is not possible to find an orifice geometric shape which will result in a linear pressure output when the metering valve port and the drain port are oriented as shown in Fig. 4(b).

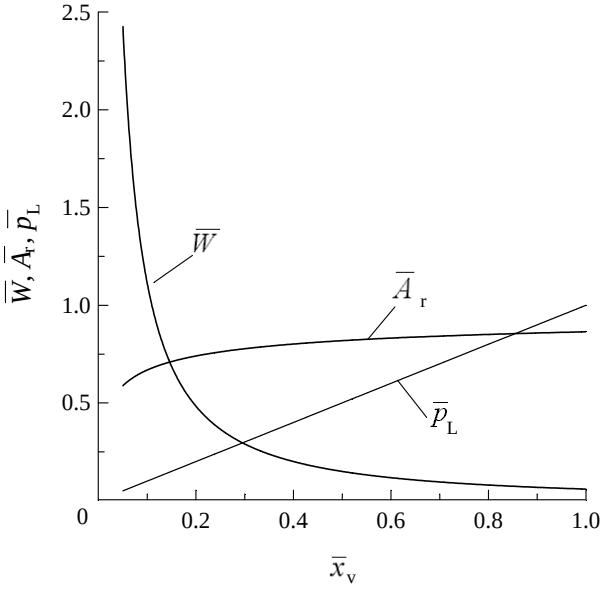

Fig. 5: *Valve port for linear pressure output*

3.2 Approximate Valve Port for Linear Pressure Output

As was mentioned, it is now necessary to find a geometry for the orifice which will approximate the curves in Fig. 5 and satisfy Eq. 13. However, if a particular orifice contour could be found which would exactly satisfy Eq. 13, it would probably be very difficult to machine. Thus some common shapes (or combination of common shapes) that would be easy to machine need to be considered. Some such possibilities are now demonstrated.

Rectangular and triangular valve port

Two very popular orifice shapes are considered: a rectangular and triangular shape. Consider first a rectangular valve port; the opening area of the metering orifice is

$$A_r = A_0 \overline{x}_v \tag{18}$$

The orifice area gradient of the valve port is thus

$$\overline{W} = \frac{A_0}{X_p} \tag{19}$$

and

$$\overline{p}_L = \frac{\overline{x}_v^2}{K(1-\overline{x}_v)^2} \tag{20}$$

The orifice area gradient of the valve port and pressure output is shown in the Fig. 6(a). It can be clearly seen that the output pressure is anything but linear. This obviously will not work. Using a triangular valve port does not improve the linearity of the output pressure much (see Fig. 6(b)). Thus these two standard configurations cannot be used.

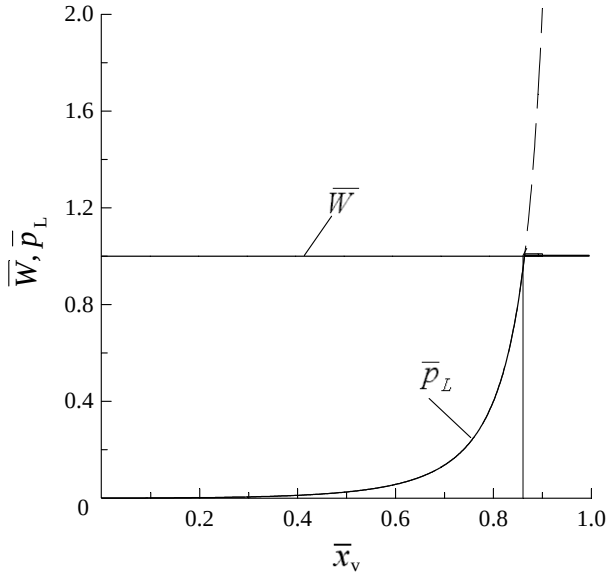

(a) rectangular valve port

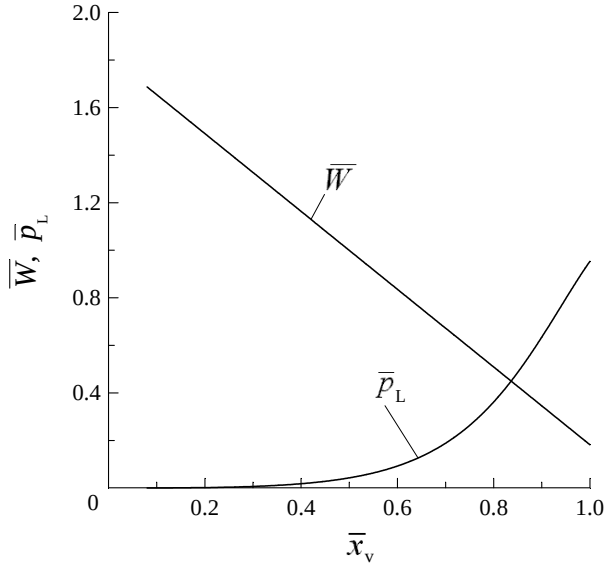

(b) triangular valve port

Fig. 6: *Output pressure of rectangular and triangular valve ports*

Multiple line segment valve port

Theoretically, it is possible to use multiple combinations of lines to approximate the shape of the metering orifices shown in Fig. 5. The more line segments, the better the approximation, but the higher the degree of machining complexity. After some study, it was

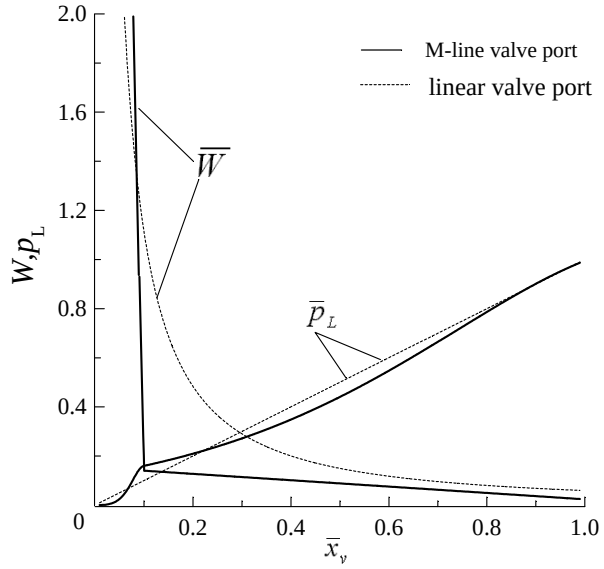

(a) $\overline{x}_{v0} = 0.1$

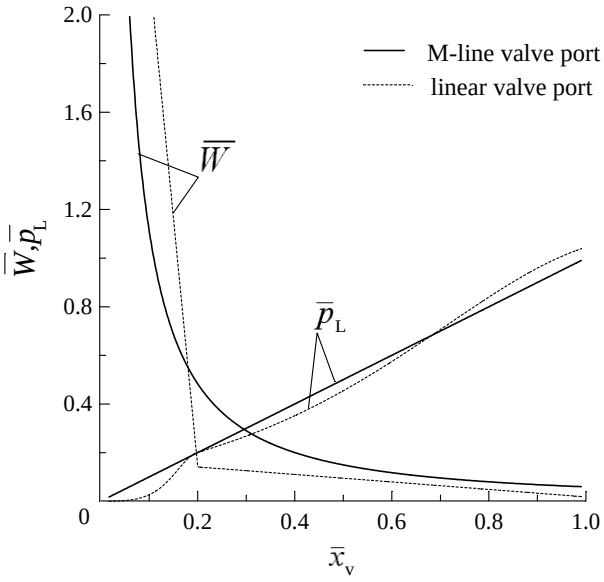

(b) $\overline{x}_{v0} = 0.2$

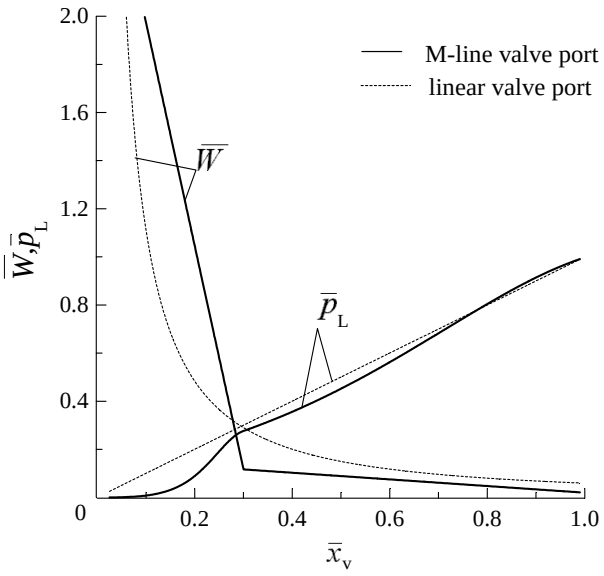

(c) $\overline{x}_{v0} = 0.3$

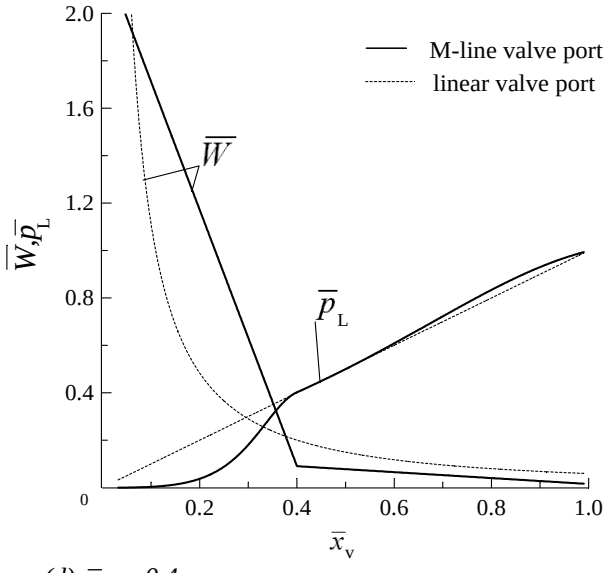

(d) $\overline{x}_{v0} = 0.4$

Fig. 7: *Output pressure of multiple line segment valve port*

decided that from a practical point of view, two line segments would be appropriate. From Fig. 5, it can be observed that for this exact shape, the opening area at small values of x_v increases rapidly, but its gradient decreases within the range 10 ~ 40 % of the spool's full displacement. Thus, two line segments with appropriate slopes were chosen to approximate the area gradient shape. Further, it was concluded that the intersection of these two line segments should occur in the region 10 ~ 40 % of the spool's full displacement ($\overline{x}_v = 1$).

Now, the slopes of the line segments must be chosen. Recall Eq. 9 and 10. At the point of the chosen intersection, the value of pressure should lie on the desired linear pressure curve. Therefore, the area defined under the first segment must be equal to the area of the exact curve. From this condition, the slope of the first segment can readily be calculated. Similarly, since the area under the second curve must also be equal to the area bounded by the exact curve, the slope of the second line segment can be obtained. Theoretically, then, the output pressure will follow a profile which is closest to the desired linear behaviour.

For different connecting points, the output pressure is shown in Fig. 7(a) - 7(d). It can be seen that if the region where the pressure is most likely to be controlled is known, then a judicious choice of the connecting point of the two segments could significantly improve the linearity of the pressure over that region.

3.3 Effect of Leakage Flow Rate

For practical applications, actuators will show some leakage. Q_L in Eq. 4 is no longer equal to zero. In this case, $Q_L = C_d a_0 \sqrt{\frac{2(p_s - p_L)}{\rho}}$ (a_0 is the equivalent leakage area) and it is assumed that the flow coefficient is equal to that of metering-in and metering-out orifice. By substituting Q_l, Q_r and Q_L into Eq. 4, the load pressure can be obtained as

$$p_L = \frac{A_r^2(x_v)}{(A_0 + a_0 - A_1(x_v))^2} \frac{K_s X_0}{A_b} \qquad (21)$$

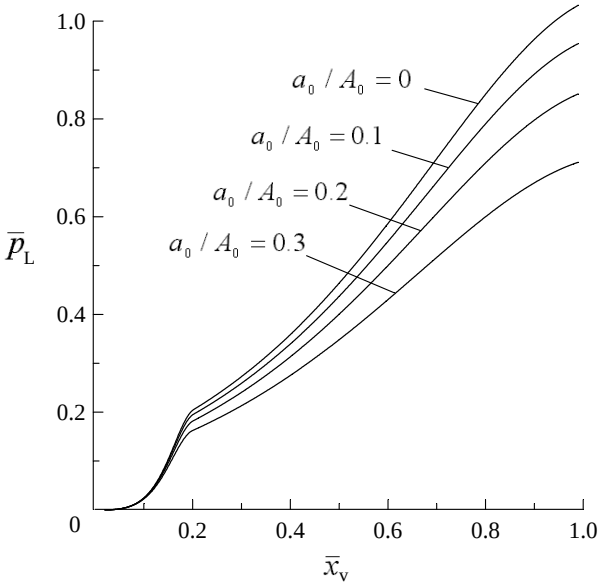

Fig. 8: *Effect of leakage flow rate*

The existence of leakage will cause the output pressure to the load to be lower than that for the case of zero leakage. For the two line segment valve port, the effect of leakage on the output pressure is shown in Fig. 8. Under some circumstances, it is possible that the required load pressure could not be achieved. The pressure reduction can be compensated for somewhat by making the maximum pressure p_{max} larger by 20 ~ 30 % of the peak load pressure. It can also be found that the maximum pressure can be extended, but at the price of reducing the effective working range to 70 ~ 80 % full spool's displacement when the leakage of the system is zero.

4 Experimental Considerations

The previous sections have considered the theoretical design of the line segments which would result in an approximately linear p_L vs x_v characteristic. It is now necessary to verify the theory using experimental data. Further, it is necessary to examine the sensitivity of the valve to changes in the operating conditions or parameters that were assumed constant or negligible in the theoretical development. Therefore, a P-Q valve was designed and experimentally tested. The P-Q valve and the experimental set-up are shown in Fig. 9. It must be pointed out that the spool shown in Fig. 9 is the same configuration as that illustrated in Fig. 3 except that in Fig. 9, the end lands are removed. The functionality of the main pool land is identical.

In the experimental study, the displacement of the spool was controlled through the use of a "2D" rotary valve (Ruan et al, 2002). In this valve a rotary displacement of the spool results in a linear motion of the spool. The rotary displacement is accomplished using a digitally controlled stepper motor. A hydraulic differential force is created by the 2D valve action which directs pressurized fluid to the end faces of the spool (A and B in Fig. 9). As illustrated in Fig. 9, a spiral groove on the left spool land and a high pressure hole on the spool have been constructed. The overlap between the hole and the groove form a variable orifice of an arm of a hydraulic bridge.

The second arm of the hydraulic bridge is a consequence of the fixed resistance of the partial spiral groove from the position of the high pressure hole to the right end of the spiral groove. The area of the right end face of the spool is designed to be one half of that of the right end face. Thus, for a balanced condition, the pressure of the left side spool chamber should be one half the system pressure, p_s. When the stepper motor rotates the spool in the direction as shown in Fig. 9, the resistance on the left hand side of the groove decreases and, hence, the pressure in the spool left chamber increases. This will result in a force imbalance across the spool and, thus, the spool will move to the right. The relative position of the pressure hole with respect to the spiral groove will decrease, increasing the resistance of the arm and decreasing the pressure. The motion continues until the pressure of the left spool chamber returns to p_s / 2 and a balance is re-established. With this arrangement, the displacement of the spool is proportional to the angular rotation of the stepper motor. The stepper motor is controlled continually with a specially developed algorithm (Ruan et al, 2000).

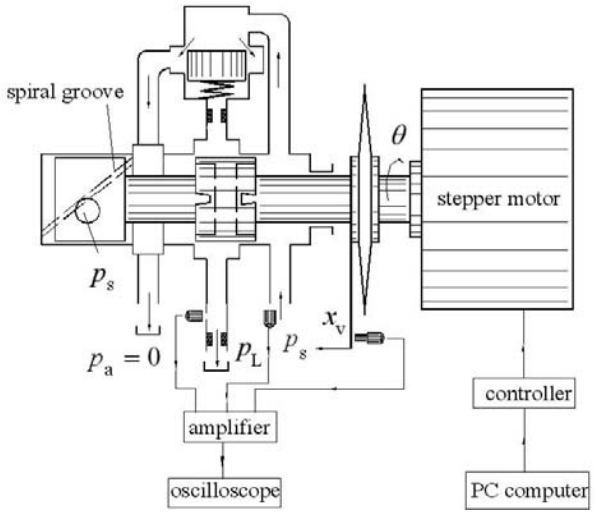

Fig. 9: *2D P-Q valve and the experimental scheme*

The special contoured valve ports are machined on the two sides of the right spool sleeve. For $0 < x_v < X_p$, the valve pressure is proportional to x_v. For $X_p \le x_v \le X_f$, the valve flow rate is proportional to x_v.

Although the valve performance in flow control is important, the behavior of the pressure as a function of x_v is that which is of concern in this paper. A pressure transducer is used to measure the output pressure of the valve and a displacement sensor is used for the axial motion of the spool. A second pressure transducer measures the inlet pressure of the valve and is used to set the maximum pressure of the system through a safety valve (relief valve). In all experiments, it was found that the

fluctuation of the pressure drop across the metering orifice (used for flow control) was less than 3 %. Thus the assumption that the spring force and Coulomb frictional force were negligible compared to the spring pretension of the bypass hydrostat is considered valid.

The angular displacement of the stepper motor (spool) was controlled using a Personal Computer. The output signals from the sensors were amplified and recorded using a digital storage scope. A small orifice block was integrated into the load port to simulate leakage in the actuator. This arrangement facilitated a study on the effects of leakage on the output pressure characteristics. The operating parameters and conditions of the experiment are listed in Table 1.

Table 1: Physical Parameters of the Experiments

Parameters/ Conditions	**Symbol**	**Value**	**Unit**
Pressure drop of bypass valve	p_s - p_l	0.52	[MPa]
System pressure	p_s	20	[MPa]
Full displacement of spool	X_p	2.2×10^{-3}	[m]
Area of full valve opening	A_0	4.3×10^{-6}	[m^2]

Several spool sleeves in which the "connecting points" of the two lines were changed - specifically at $\bar{x}_v = 0.1$, $\bar{x}_v = 0.2$ and $\bar{x}_v = 0.3$ - were machined and tested. The load theoretical pressure and its experiential counterpart as a function of x_v are shown in Fig. 10(a), (b) and (c). It can be seen from the figures that the theoretical output pressure before the connecting point has an obviously steeper slope than that after the connecting point. This difference can be attributed to the fact that several factors were not considered in the theoretical analysis; noticeably, the bypass hydrostat was assumed to be ideal and produces a constant pressure drop across the metering orifice. This is a weak assumption because small pressure variations in the Bernoulli force, spring force and Coulomb frictional force affect the force balance on the hydrostat spool and thus the pressure drop across the metering orifice shifts from its preset working point.

A second weak assumption was that relating to the statement that the flow coefficient for both the control metering orifice and the drain orifice was identical. Although the Reynolds number for both orifices changes in the same direction with pressure variation, the numerical value of the Reynolds Number and thus the flow coefficient, are different contrary to that assumed. The consequence of this would be a shift in the pressure results under some conditions which indeed is what is observed in some of the results.

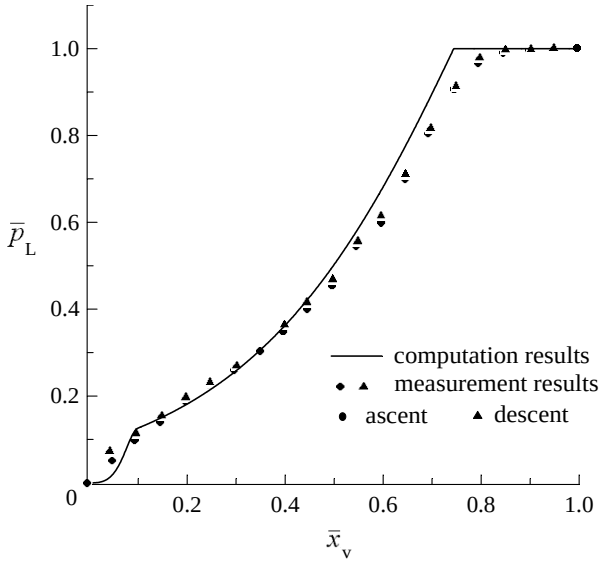

(a) $\bar{x}_v$ *= 0.1*

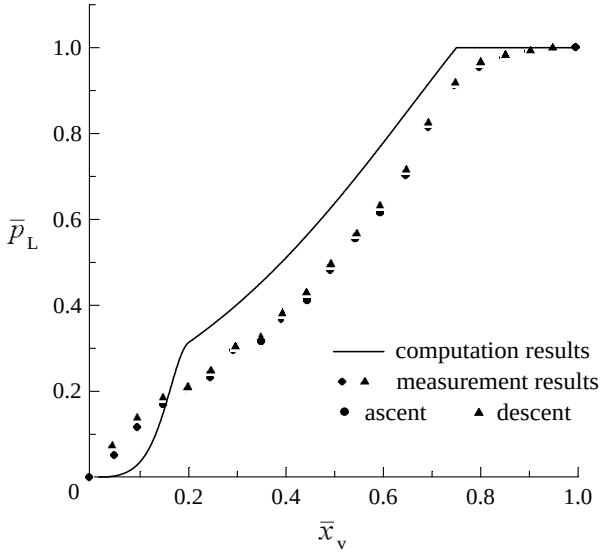

(b) $\bar{x}_v$ *= 0.2*

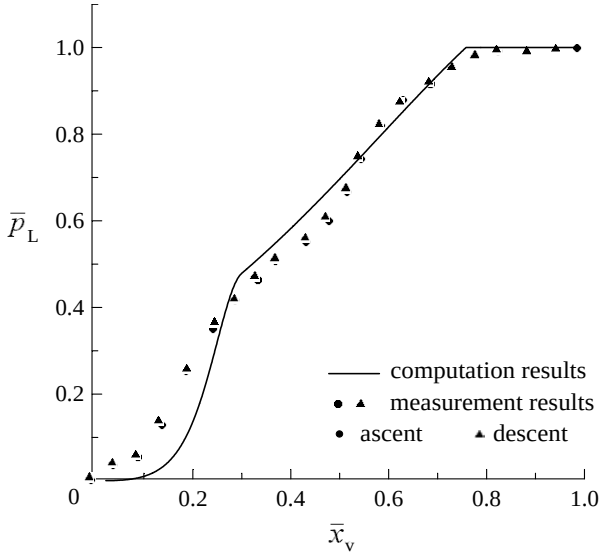

(c) $\bar{x}_v$ *= 0.3*

Fig. 10: *Output pressure as a function of* x_v

A third simplification in the model relates to the fact that the leakage flow through the clearance between the spool land and the sleeve was not taken into account in the theoretical analysis. This effect at the transition regions of the two lines can be significant. It is believed that the leakage is the main factor why the transition regions of the experimental results differ to that predicted by theory. In general, however, the theoretical results do reflect the actual experimental trends.

To illustrate the effect of leakage, the connecting point was fixed at $\bar{x}_v = 0.2X_p$ and the leakage rate increased. The measured output pressure under different leakage conditions is shown in Fig. 11. The trends predicted by theory are seen in the experimental results. As expected, leakage lowers the output pressure for the same x_v. It should be noted that for the theoretical considerations, the value of the discharge coefficient was assumed constant. In reality, this is not the case as the Reynolds number does change with x_v. Thus the differences between the theory and the experimental curves are primarily a consequence of this assumption.

To illustrate the effect of temperature on the P-x_v characteristics, the tests for zero leakage and the transition point of $\bar{x}_v = 0.2X_p$ were repeated for temperatures of 20°C, 30°C, 40°C and 50°C. The results are shown in Fig. 12. From the experimental results it is concluded that the temperature does not affect the output pressure. This is a very positive result because it was one of the design objectives for the P-Q valve. The insensitivity of the output pressure to the temperature is explained by the fact that the Reynolds number (and, hence, the discharge coefficient) at both the metering orifice and the drain sides changes in the same direction. Thus, in the hydraulic bridge, the resistances of the metering orifice and drain orifice compensate for each other; the consequence is that the output pressure becomes insensitive to variations in temperature.

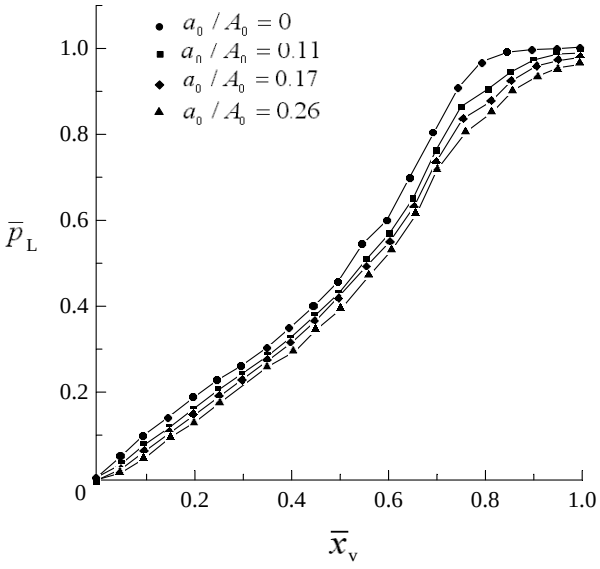

Fig. 11: *Effect of leakage flow on output pressure*

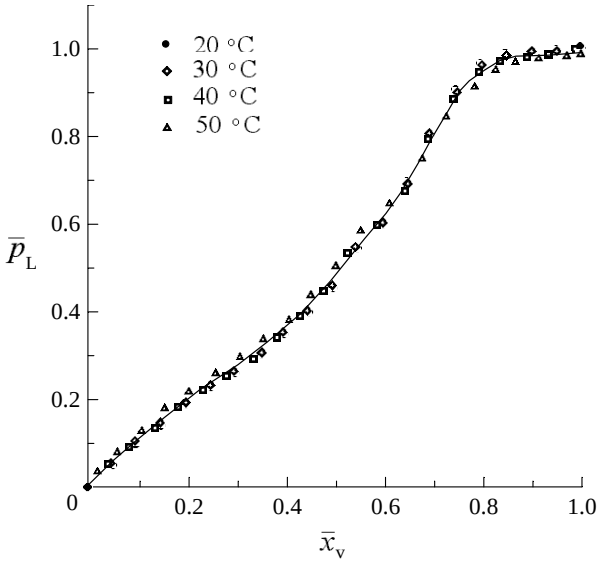

Fig. 12: *Effect of temperature on output pressure*

5 Conclusions

In the proposed P-Q valve, pressure can be controlled by constructing a hydraulic bridge within the framework of a pressure compensated flow rate control valve. In this manner, the design of the P-Q control valve is greatly simplified. The hydraulic bridge used for pressure control is achieved using a series resistance connection between a metering orifice and a drain orifice. The linearity of the output pressure, however, is highly dependent on the contour of the valve port. A theoretical analysis demonstrates that the contour of the valve port which creates a true linear pressure vs x_v characteristics is quite complex and hence would be very expensive to manufacture. An approximation to the ideal valve port contour can be created using two line segments for the valve port. An important consideration in the design of the port shapes is that the area under the first line segment should be equal to the area of the ideal contour at the connecting point of the two line segments.

The pressure control bridge was constructed using a 2D P-Q control valve scheme. The experiments were designed to measure the characteristics of the output pressure. The experimental results show that curvature of pressure vs spool displacement for the experimental valve at the different values of the connecting point are not as sharp as the theoretical predictions. This can be attributed to leakage and imperfections in the machining of the ports at the transitions points. This has an interesting side affect in that pressure linearity actually improves over that which is predicted.

Leakage flow rate at the actuator will lower the output pressure which could result in a scenario in which the controlled pressure cannot meet the maximum pressure required by the actuator. This problem is solved by setting the maximum pressure 20 ~ 30 % larger than the peak valve required.

It was also demonstrated by the experiment that the characteristics of the output pressure are insensitive to temperature change. This is because the Reynolds

number for both the metering orifice and the drain orifice changes in the same direction and, hence, the change in the resistance of these two orifices tends to compensate for each other. It is believed that the proposed flow rate and pressure control valve (P-Q valve) when used in conjunction with a 2D valve configuration is a much simpler design than that which would be used in practice, i.e. a combination of a pressure compensated flow rate control valve and a pressure limiting valve (relief or deadhead).

Acknowledgement

The authors would like to offer their gratitude to the Committee of National Foundation of Natural Sciences of China (NFNSC) and to the Natural Sciences and Engineering Research Council of Canada (NSERC) who sponsored the project. Mr. Pei and Mr. Li offered their kind helps in the course of the experiments. Gratitude is also extended to the Watch Manufacturing Factory of Hangzhou which helped machine the testing elements.

Nomenclature

a_0	Leakage area	[m^2]
A_0	Area of full opening valve port	[m^2]
A_b	Area of bypass opening valve port	[m^2]
A_r, A_l	Area of metering valve port and drain port	[m^2]
A_{sb}	End area of bypass valve spool	[m^2]
$\overline{A}_r$	Nondimensional area of valve port, $\overline{A}_r = A_r / A_0$	[-]
B_c	Coefficient of viscous frictional force	[Ns/m]
C_d	Coefficient of the flow rate	[-]
C_p	Flow-pressure coefficient of groove	[m^3/Pas]
C_q	Flow rate gain of groove	[m^2/s]
C_V	Velocity of oil flowing through valve port	[-]
F	Coulomb frictional force	[N]
p_a	Atmospheric pressure	[Pa]
p_L	Load pressure	[Pa]
p_s	System pressure	[Pa]
$\overline{p}_L$	Nondimensional load pressure, $\overline{p}_L = p_L / p_s$	[-]
Q_1	Flow rate through metering orifice	[m^3/s]
Q_2	Flow rate through drain orifice	[m^3/s]
Q_L	Flow rate to actuator	[m^3/s]
W	Width of valve port	[m]
$\overline{W}$	Nondimensional width of valve port, $\overline{W} = \frac{WX_p}{A_0}$	[-]
x_b	Displacement of hydrostat spool	[m]
X_f	Full displacement of spool for flow rate control	[m]
X_p	Full displacement of spool for pressure control	[m]
x_v	Displacement of spool	[m]
$\overline{x}_v$	Nondimensional displacement of spool, $\overline{x}_v = x_v / X_p$	[-]
θ	Rotary angle of spool	[rad/s]
ρ	Density of oil	[kg/m^3]

References

Backe W. 1973. A New Concept of Hydraulic Resistor Controlled Circuits. *Proc. of 1st National Fluid Power System and Control Conference*, pp. 312-331.

Cai, Z. S., Zhao, X. J. and **Wang, Z. Y.** 1999. Pressure Control Using Bypass Throttling. *Chinese Mecahnical Engineering*, Vol. 11, pp. 34-37.

Li, H. R. 1993. *Electro-hydraulic Control Systems*. Press of National Defense Ministry, Beijing.

Lu, Y. X., Hu, D. H. and **Wu, G. M.** 1986. *Electro-hydraulic Proportional Control*. Press of Mechanical Industry, pp. 321-324.

Ruan, J., Burton R., and **Ukrainetz, P.** 2002. An Investigation into the Characteristics of a Two Dimensional "2D" Flow Control Valve. *Journal of Dynamic System, Measurement and Control*, Transaction of ASME, Vol. 124, pp. 214-220.

Ruan, J., Ukrainetz, P. and **Burton, R.** 2000. Frequency Domain Modeling and Identification of 2D Digital Servo Valve. *International Journal of Fluid Power*, Vol. 1, No. 2, pp. 87-96.

Ruo, H. X, Li, S. L. and **Cheng, D. J.** 1993. *Electrical and Mechanical Control*. Press of Zhejiang University, Hangzhou, pp. 124-127.

Xie, R. L. 1990. *Injection Molding Machines of Plastic Materials*. Press of Machinery Industry, Beijing.

Zheng, X. R., Ye, W. B. and **Wu, P. R.** 1980. *Hydraulic Transmission*. Press of National Defense Ministry, Beijing.

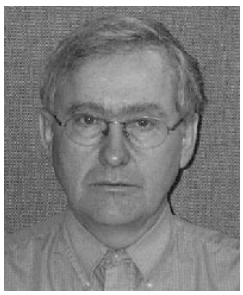

Richard Burton
P.Eng, Ph.D, Assistant Dean of the college of Engineering, Professor, Mechanical Engineering, University of Saskatchewan. Burton is involved in research pertaining to the application of intelligent theories to control and monitoring of hydraulics systems, component design, and system analysis. He is a member of the executive of ASME, FPST Division, a member of the hydraulics' advisory board of SAE and NCFP and a convenor for FPNI.

Jian Ruan
Born on April 4th 1963 in Fuan City of Fujiang Province, P.R. China. Receving Ph.D. from Harbin Institute of Technology in Sept. 1989. Active in electro-hydraulic (pneumatic) direct digital control components and systems. Post-doctoral fellow of FPTC, Zhejiang University. Professor of Mechanical Engineering at Zhejiang University of Technology

Paul Ukrainetz
BE. 1957 University of Saskatchewan, M.Sc. 1960 Univ. of British Columbia, Ph.D. 1962 Purdue University Bristol Aeroplane Co. 1957, University of Saskatchewan Assistant Professor 1962, University of Saskatchewan Associate Professor 1966, University of Saskatchewan Full Professor 1971, Head Department of Mechanical Engineering, University of Saskatchewan 1974 – 1982, Professor Emeritus 1999 - date. Active in Fluid Power Systems since 1962.